Proceedings of the 6th JFPS International
Symposium on Fluid Power, TSUKUBA 2005
November 7-10, 2005

Model of a nozzle-flapper type pneumatic servo valve and differential pressure control system design

Tao WANG*, Maolin CAI**, Kenji KAWASHIMA** and Toshiharu KAGAWA**

* Department of Mechano-Micro Engineering
Interdisciplinary Graduate school of Science and Engineering
Tokyo institute of Technology
4259 Nagatsuta-cho, Midori-ku, Yokohama, 226-8503 Japan
(E-mail: wangtao@k-k.pi.titech.ac.jp)
** Precision and Intelligence Laboratory
Tokyo institute of Technology
4259 Nagatsuta-cho, Midori-ku, Yokohama, 226-8503 Japan

ABSTRACT

In pneumatic position and force control systems, nozzle-flapper type servo valves are usually used for the pressure control. This paper proposes a linear model for a 4-port nozzle-flapper type pneumatic servo valve, which also includes the influence of the flow force, by deriving it from a full nonlinear model. The proposed linear model had a better agreement with experimental dynamics response than the former one which neglects the flow force. Furthermore, the proposed model was applied to achieve the differential pressure control between two symmetrical control chambers. A two degree-of-freedom (TDF) controller was designed based on the proposed model. The experiment results showed that differential pressure controllability could be improved for the reference input tracking and disturbance restraining by using the proposed model.

KEY WORDS

Differential pressure control, Nozzle-flapper type servo valve, Linear model, Flow force, TDF controller

NOMENCLATURE

B_f	damping coefficient of the armature-flapper	[N·m·s]
$b_{o1,\,o2}$	critical pressure ratio of the left and right fixed orifice	[--]
$b_{n1,\,n2}$	critical pressure ratio of the left and right nozzle-flapper	[--]
$C_{o1,\,o2}$	sonic conductance of the left and right fixed orifice	[s·m^4/kg]
$C_{n10,\,n20}$	sonic conductance of the left and right nozzle-flapper at zero input current	[s·m^4/kg]
$G_{c1,\,c2}$	mass flow rate of the left and right control side	[kg/s]
$G_{o1,\,o2}$	mass flow rate through the left and right fixed orifice	[kg/s]
$G_{n1,\,n2}$	mass flow rate through the left and right nozzle-flapper	[kg/s]
i	input current	[mA]
J	moment of the armature-flapper	[kg·m^2]
K_a	rotational stiffness of the flexure tube	[N·m/rad]
$K_{f1,\,f2}$	flow force cofficient of the flapper left anf right side	[N/Pa]
K_m	magnetic rotational stiffness	[N·m/rad]
K_t	torque-motor gain	[N·m/mA]
l_f	distance from the nozzle to the pivot point of the armature-flapper	[m]

$m_{o1,\,o1}$	subsonic index of the left and right fixed orifice	[--]
$m_{n1,n2}$	subsonic index of the left and right nozzle-flapper	[--]
P_a	atmosphere pressure	[Pa]
$P_{c1,\,c2}$	left and right side control pressure	[Pa]
P_s	supply pressure	[Pa]
R	gas constant	[$m^2/s^2 \cdot K$]
$V_{1,\,2}$	volume of the left and right control chamber	[m^3]
T_e	time constant due to eddy currents	[s]
T_t	torque caused by electromagnetic forces	[N·m]
x	flapper tip displacement	[m]
x_f	distance from flapper tip to each nozzle at zero input current	[m]
ΔP	differential pressure between both control sides $\Delta P=P_{c2}-P_{c1}$	[Pa]
α	armature-flapper deflection	[rad]
θ	control chamber air temperauture	[K]
ρ	air density for standard conditions	[kg/m^3]

INTRODUCTION

In many pneumatic position and force control systems, nozzle-flapper type servo valves are normally used for controlling small flow rates. For example, the air-spring type horizontal vibration isolation is mainly achieved by differential pressure control using a 4-port nozzle-flapper type pneumatic servo valve due to its simple construction, high sensitivity and wide frequency band [1]. Therefore, modeling the servo valve is important for designing a good performance control system. However, there was no general mathematic model describing a nozzle-flapper type pneumatic servo valve considering the flow force on the flapper. The nozzle-flapper type servo valve is usually treated as a proportional element with the torque motor dynamitic and the flow force being neglected. The pneumatic control system with a nozzle-flapper element is generally approximated to a first order lag system assuming an isothermal state change for the air in the load chamber [2]. The conventional control approach for differential pressure control uses a PID controller regarding the system model as a first-order model, in which parameters are recognized by experiment directly.

In this research, a full nonlinear model of the nozzle-flapper type servo valve was derived including the torque motor dynamics and the flow force. The linear model is derived through linearizing the nonlinear model around it equilibrium state. Through the simulation and experiment for the dynamics response, the influence of the flow force is confirmed. Using the proposed linear model a two-degree-of-freedom control system is designed for the differential pressure between the two load chambers.

Dynamics of servo valve and control chamber

The differential pressure control system shown in Figure 1 consists of a 4-port nozzle-flapper type electronic-pneumatic servo valve with dual fixed orifices and dual nozzles and two load chambers called as Isothermal Chambers. The armature-flapper is moved by a torque motor consisting of a coil and vertically arranged magnets. Movement of the flapper changes the distance between it and both nozzles. This creates different pressures, P_{c1} and P_{c2}, in the control sides. In the steady state, the differential pressure, $\Delta P=P_{c2}-P_{c1}$, is proportional to the input current The two Isothermal Chambers, in which the copper wires with the diameter of 50 μm are stuffed uniformly, are connected to the two control ports of the servo valve as load chambers respectively.

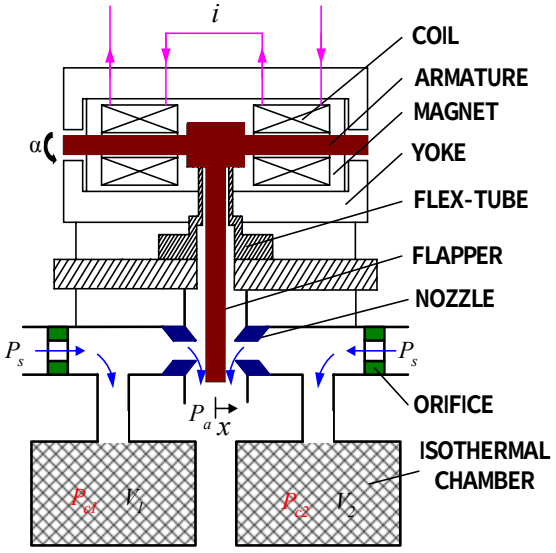

Figure 1 differential pressure control system

The toque T_t, driving the armature-flapper generated by the coil current considering the influence of the eddy current, is given as the following [3]:

$$T_e\dot{T}_t + T_t = K_m\alpha + K_i i \qquad (1)$$

The moment around the pivot of the armature-flapper around is obtained by

$$J\ddot{x}/l_f = T_t - K_a\alpha + \left(K_{f1}P_{c1} - K_{f2}P_{c2}\right)l_f - B_f\dot{x}/l_f \quad (2)$$

The first term is toque of the torque motor as Eq. (1). The second term is the torque on the armature-flapper around the pivot, caused by the flex-tube which acts as an elastic support. The third term is the torque on the flapper around the pivot, caused by flow forces which are generated by air jet from the two nozzles.

In Eq. (2), the left and right side flow force coefficients are determined by the experimental approach using the following approximant equations [5].

$$K_{f1} = \frac{K_i}{l_j}\left[a_{11} - (a_{11} - a_{12}) e^{-\left(a_{13} \frac{x_f + x}{x_f} \right)^{a_{14}}} \right] \quad (3)$$

$$K_{f2} = \frac{K_i}{l_j}\left[a_{21} - (a_{21} - a_{22}) e^{-\left(a_{23} \frac{x_f - x}{x_f} \right)^{a_{24}}} \right] \quad (4)$$

With respect to the compressibility of air, the flow state through the fixed orifice and the nozzle-flapper can be sonic or subsonic depending upon the upstream/ downstream pressure ratio. Firstly, the flow rate through the fixed orifice is given by

$$G_o = C_o \rho P_s \varphi_o(P_c) \quad (5)$$

where

$$\varphi_o(P_c) = \begin{cases} 1 & P_c / P_s \le b_o \\ \left\{ 1 - \left(\dfrac{P_c / P_s - b_o}{1 - b_o} \right)^2 \right\}^{m_o} & P_c / P_s > b_o \end{cases}$$

G_o, C_o, P_c, b_o, m_o and φ_o, for the left and right side of the flapper are identified by attaching the subscripts 1 and 2 respectively.

The flow rates through the two nozzle-flappers are given by

$$G_{n1} = C_{n10} \rho \frac{x_f + x}{x_f} P_{c1} \varphi_{n1}(P_{c1}) \quad (6)$$

$$G_{n2} = C_{n20} \rho \frac{x_f - x}{x_f} P_{c2} \varphi_{n2}(P_{c2}) \quad (7)$$

where

$$\varphi_n(P_c) = \begin{cases} 1 & P_a / P_c \le b_n \\ \left\{ 1 - \left(\dfrac{P_a / P_c - b_n}{1 - b_n} \right)^2 \right\}^{m_n} & P_a / P_c > b_n \end{cases}$$

In the above equation, φ_n P_c, b_n, and m_n, for the left and right side of the flapper are identified by attaching the subscripts 1 and 2 respectively. The nozzle-flapper critical pressure ratio and subsonic index are considering constant with the flapper displacement change.

Air temperature inside the chamber is considered constant and isothermal state during pressure and flow rate change. It is because that the high heat capability of copper wire than air and large heat area between the copper wires and air inside the chambers. So air dynamics in two load chambers are obtained from air state equation [4].

$$G_c = \frac{V}{R\theta} \dot{P}_c \quad (8)$$

Applying the continuity equation to the 4-port nozzle-flapper servo valve, the following equation can be obtained:

$$G_c = G_o - G_n \quad (9)$$

G_c, K_c, V, P_c, G_o and G_n for the left and right side of flapper are expressed by attaching the subscripts 1 and 2 respectively.

Linear model for differential pressure model

The linear model is derived from the above nonlinear model at an equilibrium state. The equilibrium states are obtained for zero input, i.e., i=0 as follows:

α_0=0, x_0=0,

P_{c10} and P_{c20} can be calculated from Eqs. (5)-(7) and (11) when the flow rate through the fixed orifice equals that through the nozzle-flapper; the flow state at the fixed orifice is subsonic and that at the nozzle-flapper is sonic.

$$C_{o1} P_s \left\{ 1 - \left(\frac{P_{c10} / P_s - b_{o1}}{1 - b_{o1}} \right) \right\}^{m_{o1}} = C_{n10} P_{c10} \quad (10)$$

$$C_{o2} P_s \left\{ 1 - \left(\frac{P_{c20} / P_s - b_{o2}}{1 - b_{o2}} \right) \right\}^{m_{o2}} = C_{n20} P_{c20} \quad (11)$$

Because the two control pressures at equilibrium are not zero, the pressure variations and flow rate variations dynamics to the input current variation derived in Appendix A, have the forms shown in Figure 2. This block diagram shows that a differential pressure control system for two fixed chambers with a nozzle-flapper type servo valve can be validly represented by a fourth order model. Furthermore, the flow force can be considered as the disturbances to flapper movement.

The specific servo valve used in the experiment system is part AS121005 as manufactured by the PSC Company. The control pressure change range is 300~400 kPa for the rated current of ±100 mA and air supply pressure of 400 kPa. The rated differential pressure is 8.6 kPa for an input current of 10 mA. The two chambers with the

effective volume of 95 cm^2, in which the copper wires with the diameter of 50 μm and weight of 0.4 kg are stuffed uniformly, are connected to the two control ports of the servo valve closely neglecting connecting section. The experiments were performed at a constant ambient temperature of 20 °C and a supply pressure of 400 kPa.

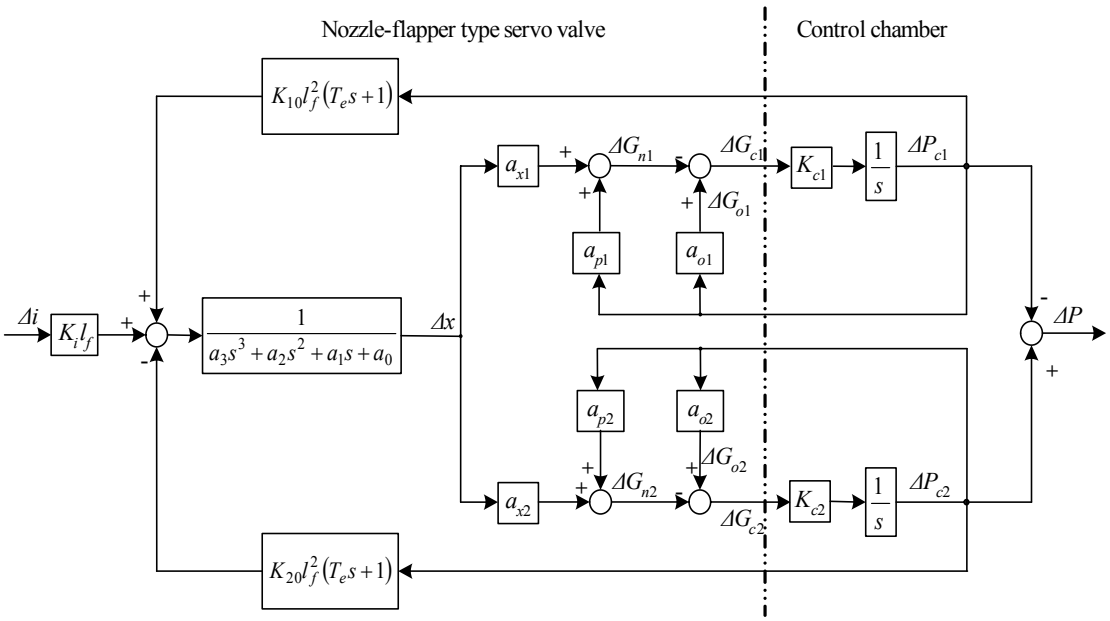

Figure 2 Schematic of a linear model for a combination of servo valve and control chambers

To validate the derived linear model, the step responses and frequency responses for the proposed model and experiment were achieved. Various step input currents were applied to the model and experimental setup. The input current was varied using step-up signals with magnitudes of ±10%, ±20% and ±30% of the rated current. There is good agreement between the results of the simulation and experiment, as shown in Figure 3. Furthermore, comparison between the results of the experiment and the simulation which neglects the flow force yields a steady state error of about 30%. This shows that flow force has the effect of reducing the pressure gain of the servo valve.

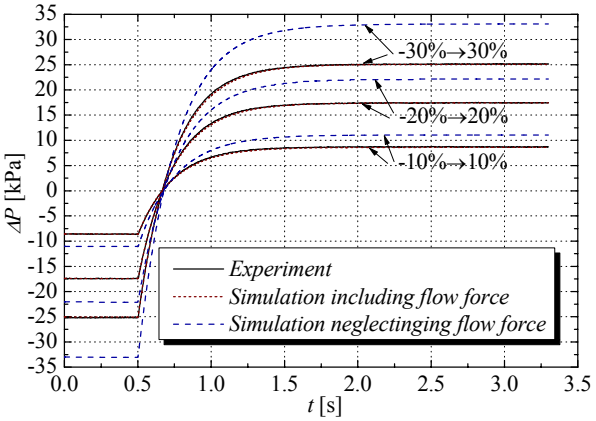

Figure 3 Step response of the differential pressure

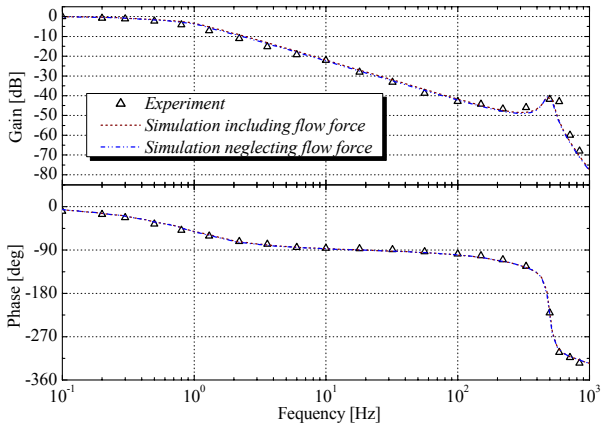

Figure 4 Frequency response of the differential pressure

The frequency response was obtained by superimposing a 5 mA swept sinusoidal current on a biased zero input current and is summarized in the bode diagram shown in Figure 4. From this bode diagram we may see that the gains for both the experiment and model descended to 3 dB at about 0.65 Hz. At about 400 Hz a peak appears in the bode diagram and corresponds to the resonant frequency of the armature-flapper. The influence of the flow force on frequency response is almost negligible. The dynamics of the system is mainly dominated by the air dynamics in the control chamber in the low frequency field. Many electro-pneumatic servo applications demand closed loop bandwidth far below

the servo valve bandwidth, therefore the dynamics of the combination of servo valve and control chambers can approximately be considered as a first order loop for the servo control design.

Control system control design

To obtain high performance control results for reference tracking and disturbance restraining simultaneously, a two degree-of-freedom (TDF) controller is designed for the differential pressure control. It comprises two components, a prefilter and a feedback compensator. The control system is shown as Figure 5.

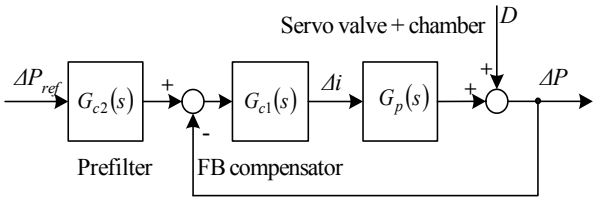

Figure 5 Differential pressure control system with a TDF controller

G_p(s) is the transfer function of the combination of servo valve and control chambers shown in Figure 2.
The FB compensator is designed as a PI controller consisting of a proportional coefficient K_p and an integral coefficient T_i:

$$G_{c1}(s) = K_p\left(1+\frac{1}{T_i s}\right) \tag{12}$$

The prefilter is designed as follows:

$$G_{c2}(s) = \frac{1+c_1c_2T_i s}{1+c_2T_i s} \tag{13}$$

Different outputs results for models, with and without flow force, with respect to input current show the flow force is mainly influencing the gain of the transfer function for servo valve show in Figure 3. Therefore the different controllers need to be designed for different models with respect to the same reference input.
In order to confirm control effect, using the models including and neglecting the flow force we designed the different controllers. The controller design is performed as the following. Firstly because the model has been established clearly shown as Figure 2, the parameters of the FB compensator can be tuned using simulating the model, no depending upon the experiment investigation, by the Critical Gain Method of Ziegler-Nichols shown as Table 1. Next the parameters of the prefilter are usually recommended as c_1=0.4 and c_2=1.35 referring to [6].

We introduced the parameters of the above two TDF controllers to the digital experimental control system respectively and compare the control results to the step input and step disturbances respectively.

Table 1 FB compensator parameters

No		K_p	T_i [s]
1	Model including the flow force	4.5	0.238
2	Model neglecting the flow force	3.375	0.270

Figure 5 shows the experiment step response using each TDF controller for a reference amplitude of 20 kPa. Better differential pressure response is achieved with the more accurate control model including the influence of the flow force and the rising time to 64% of the reference is 53 ms. Compared with it the rising time of the combination model and the control model neglecting the flow force of the servo valve are 257 ms and 73 ms respectively.

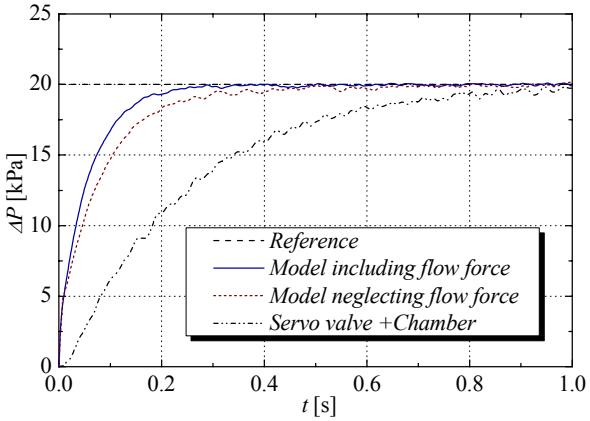

Figure 6 Step reference tracking responses

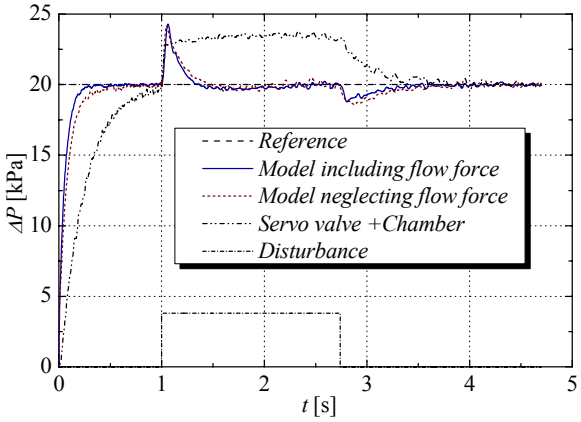

Figure 7 Disturbance restraining response

As a disturbance, an additional pressure with the amplitude of 3.7kPa and time interval of 1.74 s is added to right control chamber after the control system has settled to the steady state. Figure 7 shows that disturbance restraining response of the control model including the influence of the flow force and neglecting it at the steady state of 20 kPa. Quicker disturbance restraining effect with the control model including the influence of the flow force shows the differential pressure controllability could be improved.

Conclusion

A linear model for the differential pressure has been derived from the nonlinear model for a 4-port nozzle-flapper type pneumatic servo valve and two control chambers including the flow force of the servo valve. Simulation and experiment show that the flow force influences the steady state error of the servo valve dynamics. The differential pressure control system design using a TDF controller has been performed based on the two models including and neglecting the flow force. As expected and verified by the experiment, better control effect for reference input tracking and disturbance restraining is achieved for the proposed model including the flow force than the model neglecting it. It is signified that the differential pressure controllability can be improved by using the proposed model.

Appendix A: Derivation of the linear model

From the armature-flapper model in Eq. (1) and (2), a transfer function, relating the displacement due to input current and the control pressure can be derived as follows:

$$\frac{\Delta x(s)}{K_i l_f \Delta i(s) + (T_e s + 1) l_f^2 \left(K_{10} \Delta P_{c1}(s) - K_{20} \Delta P_{c2}(s)\right)} = \frac{1}{a_3 s^3 + a_2 s^2 + a_1 s + a_0} \quad \text{(A1)}$$

where

$a_0 = K_a - K_m$, $a_1 = B_f + K_a T_e$

$a_2 = J + B_f T_e$, $a_3 = J T_e$

K_{10} is K_{f1} at the equilibrium position.

K_{20} is K_{f2} at the equilibrium position.

By linearizing Eq. (7) at the equilibrium position, the flow rate variation at the fixed orifice can be obtained from the control pressure variation as follows:

$$\Delta G_{o1} = a_{o1} \Delta P_{c1} \quad \text{(A2)}$$

$$\Delta G_{o2} = a_{o2} \Delta P_{c2} \quad \text{(A3)}$$

where:

$$a_{o1} = \left.\frac{dG_{o1}}{dP_{c1}}\right|_{P_{c1}=P_{c10}}, \quad a_{o2} = \left.\frac{dG_{o2}}{dP_{c2}}\right|_{P_{c2}=P_{c20}}$$

By linearizing Eqs. (8) and (9) at the equilibrium position ($x=x_0=0$, $P_{c1}=P_{c10}$, $P_{c2}=P_{c20}$), the flow rate variation at the nozzle-flapper can be obtained from the displacement variation and the control pressure variation as follows:

$$\Delta G_{n1} = a_{x1} \Delta x + a_{p1} \Delta P_{c1} \quad \text{(A4)}$$

$$\Delta G_{n2} = a_{x2} \Delta x + a_{p2} \Delta P_{c2} \quad \text{(A5)}$$

where:

$$a_{x1} = \left.\frac{\partial G_{n1}}{\partial x}\right|_{\substack{x=x_0 \\ P_{c1}=P_{c10}}}, \quad a_{p1} = \left.\frac{\partial G_{n1}}{\partial P_{c1}}\right|_{\substack{x=x_0 \\ P_{c1}=P_{c10}}}$$

$$a_{x2} = \left.\frac{\partial G_{n2}}{\partial x}\right|_{\substack{x=x_0 \\ P_{c2}=P_{c20}}}, \quad a_{p2} = \left.\frac{\partial G_{n2}}{\partial P_{c2}}\right|_{\substack{x=x_0 \\ P_{c2}=P_{c20}}}$$

The transform function of the dynamics in the control chamber shown as in Eq (10) can be written as follows:

$$\Delta G_{c1}(s) = K_{c1} \Delta P_{c1}(s) \quad \text{(A6)}$$

$$\Delta G_{c2}(s) = K_{c2} \Delta P_{c2}(s) \quad \text{(A7)}$$

where:

$$K_{c1} = \frac{R\theta}{V_1}, \quad K_{c2} = \frac{R\theta}{V_2}$$

REFERENCES

1. Shearer, J. E., Study of Pneumatic Process in the Continuous Control of Motion with Compressed Air-I, II, Transactions of ASME. 1956, Feb. pp.233-249.
2. Zalmanzon, L. A., Components for Pneumatic Control Instruments, 1965, Pergamon Press.
3. Urata, E., Influence of eddy current on torque-motor dynamics, 4th IFK Workshop, 2004. Mar 24. pp. 71-82.
4. Kawashima, K. Fujita, T. and Kagawa, T., Flow Rate Measurement of Compressible Fluid using Pressure Change in the Chamber, Trans. of the Society of Instrument and Control Engineering, 2001, Vo1.1, No.1, 32, p.252-258.
5. Wang, T. Cai, M. Kawashima K and Kagawa, T., Modelling of Pneumatic Nozzle-flapper servo valves, Spring Symposium of JFPS, 2004, May 26, pp. 70-72
6. Hiroi, K., US5105138, Two degree of freedom controller, Kabushiki Kaisha Toshiba, Kawasaki, Japan, 1992, April 14.